JP2.19 The Thinning of Arctic Sea Ice, 1988-2003: Have We Passed a Tipping Point?

R. W. Lindsay* and J. Zhang
Polar Science Center, Applied Physics Laboratory
University of Washington, Seattle, Washington

1. INTRODUCTION AND BACKGROUND

The floating ice pack is a key component of the Arctic Ocean physical and biological systems. It controls the exchange of heat, water, momentum, radiative fluxes, and gases at the sea surface. Changes in the albedo of the surface brought on by changes in the ice cover over very large areas are a major element of global climate change. Through its role as a transporter of fresh water it modifies the static stability of the ocean in key areas of deep convection for the global oceans. The sea ice also blocks solar flux to the water and hence is a major control factor for primary productivity. It also acts as a support structure for organisms from phytoplankton to seals, walrus, and polar bears while limiting access to the surface for seals and whales. This component of the Arctic environment is changing rapidly.

The summer ice extent has been retreating in recent years. The summer of 2002 saw record low levels of ice extent in the Arctic (Serreze *et al.*, 2003) and the summers of 2003 and 2004 were almost as low (http://nsidc.org/data/seaice_index). This follows the very low ice extent in the western Arctic seen in the summer of 1998 (Maslanik *et al.*, 1999). This downward trend in the ice extent has been documented by a number of authors (e.g. Gloersen and Campbell, 1991; Johannessen *et al.*, 1999; Comiso, 2002). In our simulations, the mean thickness of the ice in the Arctic Ocean in 2003 is just 59% of that seen in 1987, and 2003 has the minimum mean ice thickness in the entire 56-year simulation.

2. MODEL DESCRIPTION AND DATA

We use a coupled ice/ocean model that has been used in a wide range of studies. The ice model is a multi-category ice thickness and enthalpy distribution model that consists of five main components: 1) a momentum equation that determines ice motion, 2) a viscous-plastic ice rheology with an elliptical yield curve that determines the relationship between ice deformation and internal stress, 3) a heat equation that determines ice temperature profile and ice growth or decay, 4) two ice thickness distribution equations for deformed and undeformed ice that conserve ice mass, and 5) an enthalpy distribution equation that conserves ice thermal energy (Zhang and Rothrock, 2001). The first two components are described in detail by Hibler (1979). The ice momentum equation was solved using Zhang and Hibler's (1997) numerical model for ice dynamics. The heat equation was solved, over each category, using Winton's (2000) three-layer thermodynamic model, which divides the ice in each category into two layers of equal thickness beneath a layer of snow. The ice thickness distribution equations are described in detail by Flato and Hibler (1995). The ocean model is based on the Bryan-Cox model (Bryan, 1969; Cox, 1984) with an embedded mixed layer of Kraus and Turner (1967). Detailed information about the ocean model is found in Zhang *et al.* (1998).

The model domain covers the Arctic, Barents, and Greenland-Iceland-Norwegian seas. It has a horizontal resolution of 40 km $\times$ 40 km, 21 ocean levels, and 12 thickness categories each for undeformed ice, ridged ice, ice enthalpy, and snow. The ice thickness categories, the model domain, and bottom topography can be found in Zhang *et al.* (2000). The model is forced with daily fields of sea level air pressure (SLP) and 2-m air temperature (T2m) obtained from the NCEP/NCAR Reanalysis for the 56-year period 1948 – 2003. The seasonally varying drag coefficient follows that of Overland and Colony (1994) with a minimum value of 0.97×10^{-3} in the winter and a maximum of 1.42×10^{-3} in the summer. The specific humidity and longwave and shortwave radiative fluxes are calculated following the method of Parkinson and Washington (1979) based on the SLP and T2m fields. Model input also includes river runoff and precipitation detailed in Hibler and Bryan (1987) and Zhang *et al.* (1998).

The ice concentration is assimilated from an ice concentration data set originally created by Chapman and Walsh (1993). The data set, called Gice (a more recent version is the HadISST data set, Rayner *et al.*, 1996), is obtained from the British Atmospheric Data Centre. It consists of monthly averaged ice concentration on a 1 degree grid. In the satellite era it is based largely on

* *Corresponding author's address:* Ronald W. Lindsay, Polar Science Center, University of Washington, 1013 NE 40th St., Seattle WA 98105;
e-mail: lindsay@apl.washington.edu

passive microwave measurements and in the pre-satellite era on ship reports and climatology. For 2003 only we use the HadISST ice concentrations because the Gice data set ends in 2002. We use data from 1948 – 2003 and linearly interpolate the monthly data to daily intervals.

The assimilation procedure is outlined in Lindsay and Zhang (2004). Each day the model estimate C_{mod} is nudged to a revised estimate $\hat{C}_{mod}$ with the relationship

$$\hat{C}_{mod} = C_{mod} + K(C_{obs} - C_{mod}) \qquad (1)$$

and the gain (or weighting) function is

$$K = \frac{|C_{obs} - C_{mod}|^{\alpha}}{|C_{obs} - C_{mod}|^{\alpha} + R^2} \qquad (2)$$

where C_{obs} is the observed concentration, R^2 is the error variance of the observations, and the exponent $\alpha = 6$. This large exponent means that only if the difference between the observations and the model is greater than about 0.5 are the observations heavily weighted, in effect only assimilating the ice extent. We use a fixed value of $R = 0.05$ that is consistent with the estimated errors of the Gice data set. Changes in the thickness distribution were made to accommodate the change in the ice concentration in a manner that minimized changes in the ice mass by removing or adding ice to the thinnest ice classes.

3. CHANGES IN THE MEAN THICKNESS OF LEVEL AND RIDGED ICE

In the model simulations about one third of the ice volume in the Arctic Basin is ridged ice and two thirds are level ice. Fig. 1 shows the time series of the mean ice thickness in the Arctic Ocean and the mean thickness (over the entire area) of level and ridged ice. Since 1987 the basin-wide thickness has thinned by 1.24 m or 41%. During this period the volume of ridged ice has diminished more rapidly than that of the level ice. The level ice has been on a downward trend since 1966, but the ridged ice volume peaked in 1987 and has fallen sharply since. The volume fraction of the ridged ice has fallen from 45% in 1987 to 36% in 2003. This result is consistent with the modeling study of Makshtas *et al.* (2003) who also find that most of the decrease in sea ice thickness is caused by a decrease in ridged ice and an increase in the area of undeformed ice. Rigor and Wallace (2004) explain the low summer sea ice extents of recent years as a delayed response to the high-index AO event of 1989 – 1995 and to a change of the average age of the ice in the basin, a change which would also imply a decrease in the ridged ice volume.

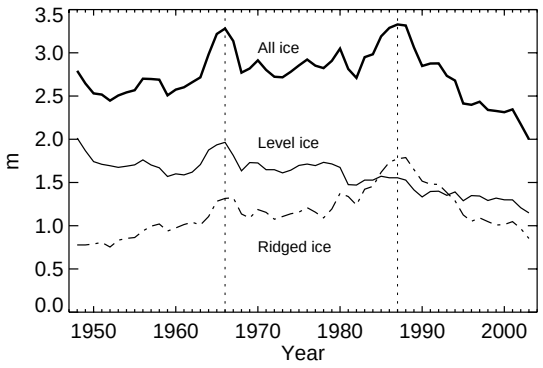

Fig. 1. Annual mean ice thickness (over the total area of the Arctic Ocean) of all ice, level ice, and ridged ice. The vertical lines indicate the times of the two principal maxima and are used in subsequent figures for reference.

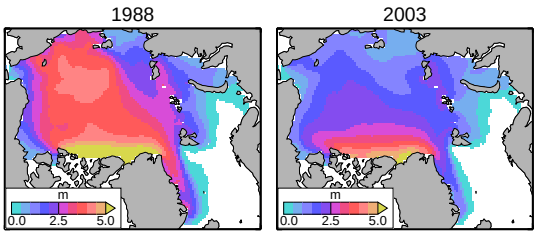

Fig. 2. Annual mean ice thickness for 1988 and 2003.

The ice has thinned over almost all of the basin. We see in Fig. 2 maps of the annual mean thickness for 1988, just after the maximum year, and for the most recent year in our study, 2003. It shows that at the beginning of the period the ice is at least 2.5 m thick over the entire central part of the basin, while in 2003 very little ice is greater than 2.5 m thick. A narrow band of thick ice remains along the Canadian coast.

The trend in the ice thickness (Fig. 3) is derived from a linear fit of the ice thickness with time and it is not the same as the difference between the first and last years divided by the time interval. It shows the greatest thinning rates are in the Beaufort Sea and along the Canadian coast. There is a significant reduction in the ridged-ice volume all along the Alaskan, Canadian, and Greenland coasts while the level-ice volume was reduced only slightly in the same period. The change in the mean thickness is almost all due to the change in ridged ice.

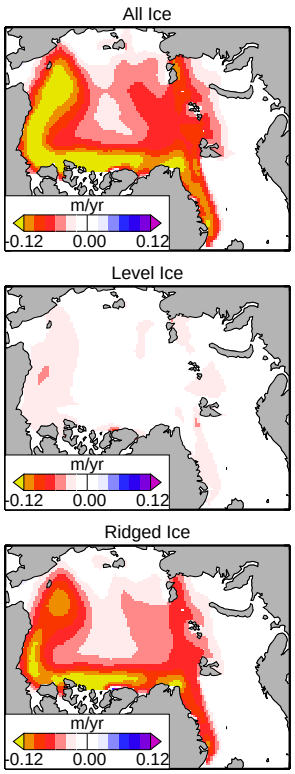

Fig. 3. Trend in the ice thickness for the sixteen-year period 1988-2003 for all ice, level ice, and ridged ice.

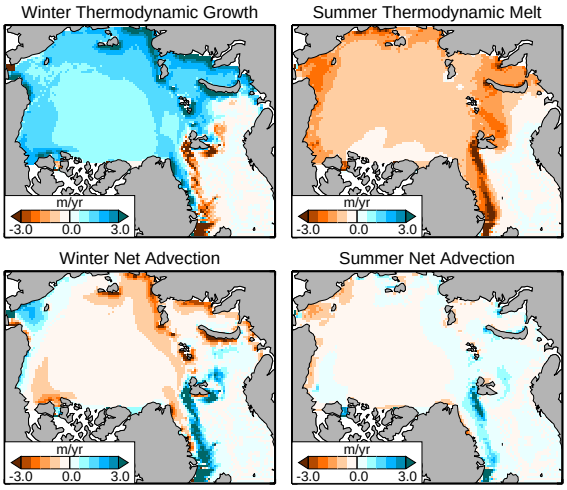

Fig. 4. Mean annual thickness changes due to thermodynamic growth or melt and net advection per year for winter (October through April) and summer (May through August) for the 56-year period 1948 to 2003.

4. PROCESSES CONTRIBUTING TO ICE THICKNESS CHANGE

4.1. Advection and thermodynamic growth

Monthly changes in the ice thickness at each grid cell can be partitioned into two components, one due to the net advection or mass-flux convergence,

$$\Delta h_{adv} = -(\nabla \cdot \bar{h}\mathbf{u})\Delta t \quad , \qquad (3)$$

where **u** is the vector velocity, $\bar{h}$ is the mean ice thickness, and Δt is the time interval (one month); and one due to thermodynamic growth or melt,

$$\Delta h_{tdg} = \Delta t \sum g(h)[f(h) + \phi(h)] \quad , \qquad (4)$$

where the summation is over the thickness bins and $g(h)$ is the thickness distribution, $f(h)$ is the thermodynamic growth rate, and $\phi(h)$ is the lateral melt rate. The net thickness change is then

$$\Delta h = \Delta h_{adv} + \Delta h_{tdg} \qquad (5)$$

These terms of the ice mass balance have significant spatial and seasonal variability, as might be expected. Fig. 4 shows the mean annual change in the thickness due to each of the two terms for the winter and summer seasons from the 56-yr simulation. There is net growth of 1 m or more over much of the basin in the winter and a lesser amount of melt in the summer. The net advection is quite small but slightly negative over most of the central part of the basin due to a small net divergence. The region of greatest winter growth is in the Laptev Sea and in portions of the Kara and Barents seas where more than 3 m of ice grows each winter. These are locations where there is often significant off-shore flow and the continual creation of shore polynyas. Because of the winter off-shore flow, the western Laptev is also a region of net advective loss in the winter but not in the summer when the winds are more variable. The eastern edge of the East Greenland Current exhibits strong advective gain in both winter and summer, as well as strong melt in both seasons. Another region of strong advective gain in the winter is in the Chukchi Sea, where the anticyclonic Beaufort Gyre brings thicker ice into the shelf region. Similarly, an advective loss is seen in the eastern Beaufort Sea, where the gyre is pulling thick ice away from the coast.

These terms also show significant interannual variability. Fig. 5 shows the time series of the annual total thermodynamic growth and net export for winter and summer averaged over the Arctic Ocean. The top panel shows an average net winter growth of 1.30 m yr^{-1} and an average summer melt of –0.91 m yr^{-1}. The net advection is nearly zero in the summer and negative in the winter, averaging –0.41 m yr^{-1}. This term repre-

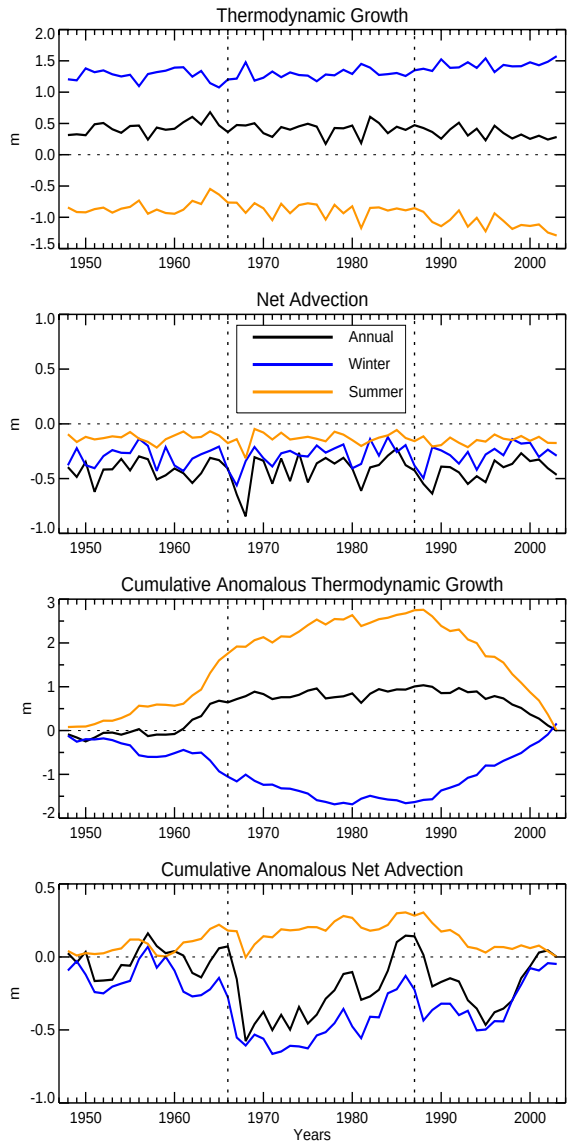

Fig. 5. Time series of the thermodynamic growth and net advection for the winter (October – April), summer (May – September), and the whole year, averaged over the Arctic Ocean. The top two panels show the yearly net thickness changes and the bottom two show the cumulative effect of anomalies from the mean for each parameter.

sents the net export of ice from the basin. The average thinning rate due to both processes over the entire 56-yr period is –0.02 m yr^{-1}.

The net change in the ice thickness is determined by the difference in the cumulative effect of large terms. Over the 56 years of simulation, the total thermodynamic winter growth amounts to 73 m of ice. This is balanced by summer melt and net advection to produce a net change of just –1 m (Figure 1). So how, when, and where is the net change produced? To determine the integrative effect of anomalous periods of thickness change contributed by each of these terms we compute the cumulative anomaly from the mean. This type of plot simply shows periods when one of the terms is contributing more or less than normal to the change of the ice thickness. When the line is sloping upward (positive anomalies) the term is contributing to thickening of the ice more than average (either through more growth, less melt, or less advective loss than average) and when the line is sloping down it is contributing to thinning of the ice more than average (either through less growth, more melt, or more advective loss than average). By definition these plots must begin and end at zero. A consistent upward trend in one of the terms will appear as first a downward sloping line (the anomalies are negative) and then an upward sloping line (the anomalies are positive). A long-term trend in the mean ice thickness is not represented in these anomalies, since it is due to an imbalance of the mean values of the mass balance terms.

The bottom two panels in Fig. 5 show the cumulative anomalies of the thermodynamic and advective terms. The sum of the annual lines in these two plots reproduces the shape of the mean ice thickness line in Fig. 1 without the 56-yr trend. The summer melt anomalies represent the largest contribution to the cumulative interannual variability of the thickness changes. There was a sharp decrease in the summer melt (upward trending line) in the early sixties contributing to the 1966 ice thickness maximum. The summer melt was generally less than average until 1987. The cumulative effect amounts to 2.5 m. After 1988 the melt was generally greater than average (downward trending line). The winter freezing rates mirror, to a certain extent, the summer melt anomalies because when there is high summer melt and increased thin ice or open water extent, the ice production rate in the these regions in the following winter is much larger. The net anomalous thermodynamic growth (black curve in Figure 5c) leads to a thickening in the early sixties and then little change until mid 1990's when the net change produces a thinning of the ice of about 1 m in the final few years of the study period.

We see that the two maxima in the ice thickness (Fig. 1) are characterized by different processes. Before 1966 there is a sharp decrease in the summer melt rate and a modest decrease in the net advective loss leading to an increase in the thickness. After 1966 a sharp increase in the advective loss and little change in the thermodynamic terms lead to a sharp drop in the thickness. Before the 1987 maximum there is little change in the sum of the thermodynamic terms, however there is a sharp decrease in the advective loss before the maximum and then afterwords a sharp increase. This increase in the advective loss, coupled with a coordi-

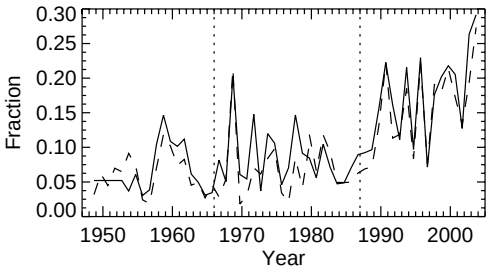

Fig. 6. September open water extent as a fraction of the area of the Arctic Ocean. The extent is the area with ice concentration less than 0.15. The solid line is from the Gice observations and the dashed line is from the model simulations.

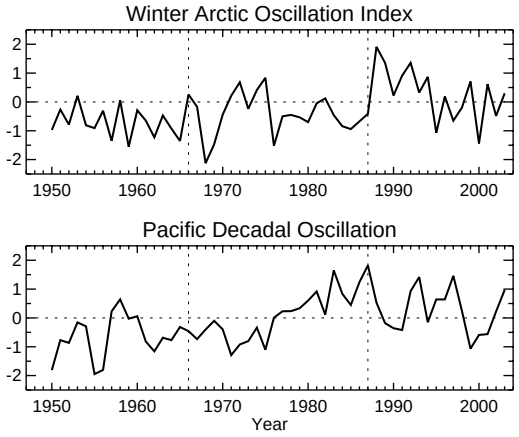

Fig. 7. Time series of the winter average (November - March) Arctic Oscillation index and the annual average Pacific Decadal Oscillation index. The AO data are from the NOAA Climate Prediction Center and the PDO data are from N. Mantua (jisao.washington.edu/pdo).

nated shift in the two atmospheric circulation indexes that created extensive areas of open water, is the trigger for beginning the sustained loss of ice in the Arctic Ocean. It is a reflection of the surge of old ice lost from the ocean that Rigor and Wallace (2004) refer to during this time period.

The first year of extensive open water is in 1990, after the strong advective loss of ice in 1989. Fig. 6 shows the September open water fraction in the Arctic Ocean from the Gice data set as well as from the model simulation. The two match well because of the data assimilation procedures for ice concentration. For both the 1966 maximum and the 1987 maximum, the open water expanded greatly about three years after the maximum and after the main pulse of advective loss occurred. The figure shows the remarkable increase in the late summer open water extent in the nineties and shows that the last year of the record, 2003, had the greatest open water extent, measured as a fraction of the area of the Arctic Ocean, in the entire record. This record year is different from the 2002 record minimum ice extent reported by Serreze *et al.* (2003) because here we are looking at only the Arctic Ocean ice extent and not that of the Canadian Archipelago or the Barents and Kara seas. The mean open water over the Arctic Ocean has greatly increased in the last 16 years, but the trend is frequently broken by years with reduced open water.

4.2. Atmospheric indexes

In Fig. 5 the net effects of anomalies in advection are smaller than anomalies in thermodynamics and do not exceed 1 m. There is, however, a period of less than average winter advective loss (upward sloping line) before the two maxima in 1966 and 1987 and more than average advective loss (downward sloping line) after each one. Curiously, the advective loss after the 1966 maximum is associated with a negative Arctic Oscillation index (AO, Thompson and Wallace, 1998) while that after the 1987 maximum is associated with a positive AO index. Fig. 7 shows the time series of the winter AO and the annual average of the Pacific Decadal Oscillation (PDO, Mantua *et al.*, 1997). The PDO is particularly important for processes in the Pacific sector of the basin. In the two years after the maximum in 1987 the AO shifts from slightly negative to an extreme positive mode while the PDO shifts from a very positive mode to a slightly negative one. This coordinated shift in the two major indexes related to the atmospheric circulation in the Arctic Ocean is not seen in the rest of the record and is quite distinct from what happens after the 1966 maximum. The shift in the atmospheric indexes caused a shift in the location and strength of the Beaufort Gyre and the creation of large extents of summer open water, beginning in 1990.

4.3. Air temperatures

The air temperature over the Arctic Ocean has gradually warmed about 5˚C in the winter over the 56-yr period of the study but has not changed significantly in the other seasons with the exception of the most recent 16-yr period. The atmosphere has responded to the thinning ice by warming in the fall, when the new ice is thinnest. The rate of warming is clearly greater than in winter or spring, when the ice has grown sufficiently thick to cool to more normal temperatures. Fig. 8 shows the seasonal trends in the 2-m air temperature in the 16-yr period 1988-2003. The warming over the Arctic Ocean in the fall is considerable and the warming persists into

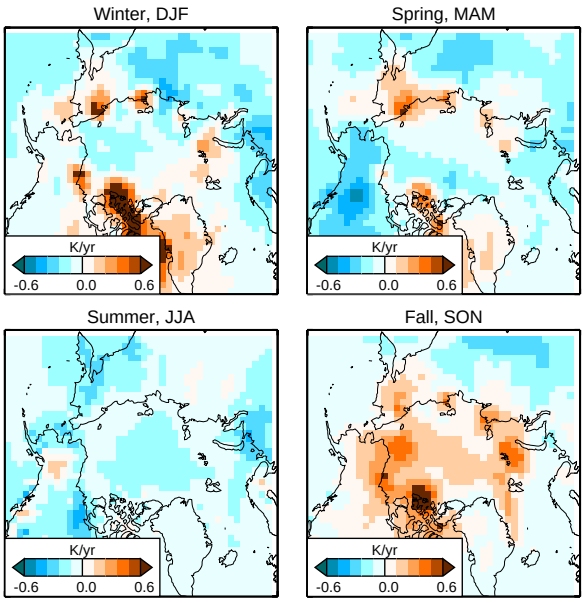

Fig. 8. Seasonal trends in the 2-m air temperature from the NCEP Reanalysis for the 16-year period

the winter and spring months in isolated areas. Much of the land area shows marked cooling, particularly in the spring over western North America. Note this air temperature is a forcing for the model, not a model result, and is directly tied to buoy and land station observations through the Reanalysis effort. The patterns of recent warming shown here are quite different from what Rigor *et al.* (2000) found for the 19-yr period 1979–1997 that included years before the ice maximum. They showed the strongest warming in the spring. However the results are consistent with simulations of climate change in the Arctic performed by climate models which also show maximum warming over the Arctic Ocean in the fall under increased-greenhouse-gas scenarios (Moritz *et al.* 2002).

The increased melt in the summer is closely related to changes in the duration of the melt season. Belchansky *et al.* (2004) find that passive-microwave-based estimates of the duration of the melt season were longer in the period 1989–2001 compared to 1979–1988. The mean duration of the melt season was largest in 1989, just after the winter AO index was at its highest and near the beginning of the recent thinning. They find that the increase in the melt season length is greatest in the northern Chukchi Sea, near the area where there has been increased summer open water extent. They also find that despite recent declines in the winter AO index, the melt duration has not returned to the values seen before 1988 nor have the spatial patterns in the melt duration returned to those seen in the 1979–1988 low-index AO period.

Our analysis of the melt-season duration based on the NCEP Reanalysis 2-m air temperature forcing data indicates that the average melt-season duration over the Arctic Ocean has increased by 6 days between the two 16-year periods 1972–1987 and 1988–2003. However the trend in the melt season duration in the later period is back toward the mean value for the entire 56-year period after a record-long season in 1989. This is different from what the passive microwave-based estimates of the surface-melt duration suggest. Perhaps the increased heat flux from the ocean to the surface through thinning ice has caused the surface to melt earlier even with similar 2-m air temperatures, so that the change in the melt-season duration is not only a function of the air temperature but also of the ice thickness and snow depth.

5. COMMENTS & CONCLUSIONS

The main points and conclusions made in this study include:

- Sea ice in the Arctic Ocean has thinned dramatically since 1987 in our simulations and the summer ice extent, both in observations and in the model, is greatly reduced since that date. The maximum basin-wide ice thickness was seen in 1966 and a secondary maximum occurred in 1987 followed by a large and consistent decrease in the mean thickness through 2003. The thinning rate is greatest in the Alaska-Canada-Greenland sector.
- The basin-wide average change in the thickness is usefully partitioned between winter and summer thermodynamic growth or melt and net advection. The largest source of variability is in the summer melt, which shows a consistent trend of increasing melt over the 56-year study period and a marked increase in the melt trend in the last 16 years. Winter freezing rates mirror the summer melt rates -- when there is increased summer melt and open water creation there is increased winter ice production.
- The decreasing trend in the mean ice thickness is caused primarily by thermodynamic processes in the Chukchi, Beaufort, Greenland seas and in Fram Strait while advective processes dominate north of Canada and Greenland.
- The winter air temperature over the Arctic Ocean has gradually warmed over the 56-yr period leading to a reduced equilibrium ice thickness. In the last 16 years the air temperature over the Arctic Ocean has not changed much except in the fall, when there is considerable warming. This warming we attribute to the thinning ice cover which allows more heat from the ocean to warm the air, the additional heat having been absorbed through open water in the summer.

- The two primary indexes for atmospheric circulation in the Arctic, the AO and the PDO, both exhibited a sudden and large shift in mode in 1989, just after the 1987 ice maximum. A spike in the AO index in late 1980's and early 1990's caused a flushing of some of the old, thick ridged ice. The AO and PDO indexes have returned to near normal values since the mid 1990's, yet the simulated thinning continues unabated.

The thinning of the ice cover has multiple linked causes: 1) the winter air temperature has gradually warmed, leading to a reduced equilibrium ice thickness; 2) a sudden temporary shift in two principal atmospheric indexes caused a flushing of some of the older thicker ice and the creation of increased summer open water by shifting the strength and location of the Beaufort Gyre; 3) the increasing amounts of summer open water allowed for increasing absorption of solar radiative fluxes; 4) the large extents of summer open water caused thinner first-year ice to be created because of the additional heat absorbed by the ocean; and finally 5) the thinner first-year ice is often entirely melted by the end of the subsequent summer.

It is quite possible that the large changes initiated by the gradual winter warming and the atmospheric circulation anomalies of the early 1990's have tipped the system into a new equilibrium state in which very large extents of summer open water and winter first-year ice are the norm. The system may be approaching a new quasi-stable state in which there is much more melt and open water in the summer, much more first year ice growth (and melt), and less ridged ice. The old regime may not be regained until there is either a prolonged cooling or a prolonged period of very negative AO index that can once again build the reservoir of thick ridged ice by strengthening the circulation of the Beaufort Gyre. The gradually increasing winter air temperatures, unrelated to the most recent ice thinning and fall warming, may be reflecting a global warming signal that will preclude a return to the old regime.

ACKNOWLEDGEMENTS

The NCEP Reanalysis data were obtained from the National Center for Atmospheric Research. The Gice and HadISST data sets were obtained from the British Atmospheric Data Center. The AO data are from the NOAA Climate Prediction Center and the PDO data are from N. Mantua (jisao.washington.edu/pdo). We gratefully acknowledge helpful discussions with D. Rothrock, A. Schweiger., and M. Steele. This work was supported by the NASA Cryospheric Sciences Program, the NOAA Arctic Research Program, and the NSF Office of Polar Programs. This activity is part of the Arctic Sea Ice-Ocean Reanalysis (ASOR) Project which seeks to determine the historical states of the ice/ocean system using a range of modeling and data assimilation methods.

REFERENCES

Belchansky, G. I., D. C. Douglas, and N. G. Platonov, 2004: Duration of the Arctic sea ice melt season: regional and interannual variability, 1979-2001. *J. Climate*, **17**, 67–80.

Bryan, K., 1969: A numerical method for the study of the circulation of the world oceans. J. *Comput. Physics*, **4**, 347–376.

Chapman, W. L., and J. E. Walsh, 1993: Recent variations of sea ice and air temperatures in high latitude. *Bull. Amer. Meteor. Soc.*, **71**, 33-47

Gloersen, P., and W. J. Campbell, 1991: Recent variations in Arctic and Antarctic sea-ice covers. *Nature*, 352, 33-36.

Comiso, J. C., 2002: A rapidly declining perennial sea ice cover in the Arctic. *Geophys. Res. Lett.*, **29**, doi:1029/2002GL015650.

Cox, M.D., 1984: *A primitive equation, three-dimensional model of the oceans*, GFDL Ocean Group Tech. Rep. No. 1, Geophys. Fluid Dynamics Lab./NOAA, Princeton Univ., Princeton, NJ.

Flato, G. M., and W. D. Hibler III, 1995: Ridging and strength in modeling the thickness distribution of Arctic sea ice. J. Geophys. Res., 100(C9), 18,611-18,626.

Hibler, W. D. III, 1979: A dynamic thermodynamic sea ice model. J. Phys. Oceanogr., 9, 817-846.

Hibler, W. D. III, and K. Bryan, A diagnostic ice-ocean model. *J. Phys. Oceanogr.*, *7*, 987–1015, 1987.

Johannessen, O. M., E. V. Shalina, M. W. Miles, 1999: Satellite evidence for an Arctic sea ice cover in transformation. *Science*, **286**, 1937–1939.

Kraus, E.B., and J.S. Turner, A one-dimensional model of the seasonal thermocline: II. The general theory and its consequences. *Tellus*, **19**, 98–106, 1967.

Lindsay, R. W. and J. Zhang, 2004: Assimilation of Ice Concentration in an Ice/Ocean Model, *J. Atmos. Ocean. Tech.*, submitted (pdf file at psc.apl.washington.edu/lindsay/pdf_files/ic_assimilation.pdf).

Makstas, A. P., S. V. Shoutilin, and E. L. Andreas, 2003: Possible dynamic and thermal causes for the recent decrease in sea ice in the Arctic Basin. *J. Geophys. Res.*, **108**(C7), 3232, doi: 1029/1001JC000878.

Mantua, N. J., S. R. Hare, Y. Zhang, J. M. Wallace, and R. C. Francis, 1997: A Pacific Interdecadal Climate Oscillation with Impacts on Salmon Production, *Bullet. Amer. Met. Soc.*, **78**, 1069–1079.

Maslanik, J. A., M. C. Serreze, and T. Agnew, 1999: On the record reduction in the western Arctic sea-ice cover in 1998. *Geophys. Res. Lett.*, **26**, 1905–1908.

Moritz, R. E., C. M. Bitz, and E. J. Steig, 2002: Dynamics of Recent Climate Change in the Arctic, *Science*, **297**, 1497–1502.

Overland, J. E. and R. L. Colony, 1994: Geostrophic drag coefficients for the central Arctic derived from Soviet drifting station data. *Telus*, **46A**, 75–85.

Parkinson, C.L. and W.M. Washington, 1979: A large scale numerical model of sea ice. J. Geophys. Res., 84, 311–337, 1979.

Proshutinsky, A.Y. and M.A. Johnson. 1997: Two circulation regimes of the wind-driven Arctic Ocean. *J. Geophys. Res.*, **102**(C6), 12493--12514.

Rayner, N. A., E. B. Horton, D. E. Parker, C. K. Folland, and R. B. Hacket, 1996: *Version 2.2 of the global sea-ice and sea surface temperature data set, 1903-1994*. Hadley Centre for Climate Prediction and Research, Climate Res. Tech. Note 74, 21 pp.

Rigor, I., R. Colony, and S. Martin, 2000: Variations in Surface Air Temperature Observations in the Arctic, 1979 - 1997. *J. Climate*, **13**, 896–914.

Rigor, I.G. and J. M. Wallace, 2004: Variations in age of Arctic sea ice and summer sea-ice extent, *Geophys. Res. Lett.*, **31**, L09401, doi:10.1029/2004GL019492.,

Rothrock, D.A., Y. Yu, G.A. Maykut, 1999: Thinning of the arctic sea-ice cover, *Geophys. Res. Lett.*, **26**(23), 3469-72.

Rothrock, D. A., J. Zhang, and Y. Yu, 2003: The arctic ice thickness anomaly of the 1990s: A consistent view from observations and models. *J. Geophys. Res,* **108**(C3), doi:10.1029/2001JC001208.

Serreze, M. C., J. A. Maslanik, T. A. Scambos, F. Fetterer, J. Stroeve, K. Knowles, C. Fowler, S. Drobot, R. G. Barry, and T. M. Haran, 2003: A record minimum arctic sea ice extent and area in 2002. *Geophys. Res. Let.*, **30**, 1110, doi:10.1029/2002GL016406.

Thompson, D. W. J, and J. M. Wallace, 1998: The Arctic Oscillation signature in the wintertime geopotential height and temperature fields. Geophys. Res. Lett., 25, 1297-1300.

Winton, M., A reformulated three-layer sea ice model. *J. Atmos. Ocean. Tech.,* 17, 525–531, 2000.

Zhang, J., and W.D. Hibler, 1997, On an efficient numerical method for modeling sea ice dynamics, J. Geophys. Res., 102, 8691-8702.

Zhang, J., D.A. Rothrock, and M. Steele. 2000. Recent changes in Arctic sea ice: The interplay between ice dynamics and thermodynamics, *J. Climate*, **13**, 3099–3114.

Zhang, J. and D.A. Rothrock: A thickness and enthalpy distribution sea-ice model, J. Phys. Oceanogr., 31, 2986-3001, 2001.

Zhang, J., W.D. Hibler, III, M. Steele, and D.A. Rothrock, 1998: Arctic ice-ocean modeling with and without climate restoring, *J. Phys. Oceanogr.*, **28**, 191